NEOPLASIA
www.neoplasia.com

Volume 20 Number 9 September 2018 pp. 883–893 883

Mutational Intratumor Heterogeneity is a Complex and Early Event in the Development of Adult T-cell Leukemia/Lymphoma

Amir Farmanbar[*,†,1], Sanaz Firouzi[*,1], Wojciech Makałowski[‡], Robert Kneller[§], Masako Iwanaga[¶], Atae Utsunomiya[#], Kenta Nakai[*,†] and Toshiki Watanabe[*,]**

[*]Department of Computational Biology and Medical Sciences, Graduate School of Frontier Sciences, The University of Tokyo, Tokyo, Japan; [†]Human Genome Center, The Institute of Medical Science, The University of Tokyo, Tokyo, Japan; [‡]Institute of Bioinformatics, Faculty of Medicine, University of Muenster, Germany; [§]Research Center for Advanced Science and Technology, The University of Tokyo, Tokyo, Japan; [¶]Department of Frontier Life Science, Graduate School of Biomedical Sciences, Nagasaki University, Nagasaki, Japan; [#]Department of Hematology, Imamura General Hospital, Kagoshima, Japan; [**]Department of Advanced Medical Innovation St. Marianna University Graduate School of Medicine, Kanagawa, Japan

Abstract

The clonal architecture of tumors plays a vital role in their pathogenesis and invasiveness; however, it is not yet clear how this clonality contributes to different malignancies. In this study we sought to address mutational intratumor heterogeneity (ITH) in adult T-cell leukemia/lymphoma (ATL). ATL is a malignancy with an incompletely understood molecular pathogenesis caused by infection with human T-cell leukemia virus type-1 (HTLV-1). To determine the clonal structure through tumor genetic diversity profiles, we investigated 142 whole-exome sequencing data of tumor and matched normal samples from 71 ATL patients. Based on SciClone analysis, the ATL samples showed a wide spectrum of modes over clonal/subclonal frequencies ranging from one to nine clusters. The average number of clusters was six across samples, but the number of clusters differed among different samples. Of these ATL samples, 94% had more than two clusters. Aggressive ATL cases had slightly more clonal clusters than indolent types, indicating the presence of ITH during earlier stages of disease. The known significantly mutated genes in ATL were frequently clustered together and possibly coexisted in the same clone. *IRF4*, *CCR4*, *TP53*, and *PLCG1* mutations were almost clustered in subclones with a moderate variant allele frequency (VAF), whereas *HLA-B*, *CARD11*, and *NOTCH1* mutations were clustered in subclones with lower VAFs. Taken together, these results show that ATL displays a high degree of ITH and a complex subclonal structure. Our findings suggest that clonal/subclonal architecture might be a useful measure for prognostic purposes and personalized assessment of the therapeutic response.

Neoplasia (2018) 20, 883–893

Abbreviations: ATL, Adult T-cell Leukemia/Lymphoma; HTLV-1, Human T-cell Leukemia Virus Type-1; PVL, Proviral Load; NGS, Next Generation Sequencing Technology; WES, Whole Exome Sequencing; SNV, Single Nucleotide Variation; CNA, Copy Number Alteration; VAF, Variant Allele Frequency; ITH, Intratumor Heterogeneity.

Address all correspondence to: Prof. Toshiki Watanabe, Department of Advanced Medical Innovation, St. Marianna University Graduate School of Medicine, Miyamae-ku, Kawasaki, Kanagawa Prefecture, 216-8511, Japan, E-mail: tnabe@ims.u-tokyo.ac.jp or Dr. Sanaz, Firouzi 3rd floor, 2nd building, The Institute of Medical Science, Shirokanedai Campus, The, University of Tokyo, 4-6-1 Shirokanedai, Minato-ku, Tokyo 108-8639, Japan. E-mail: firouzisanaz1@gmail.com

Received 14 April 2018; Revised 2 July 2018; Accepted 6 July 2018

1476-5586
https://doi.org/10.1016/j.neo.2018.07.001

Introduction

Intratumor Heterogeneity in Adult T-cell Leukemia/Lymphoma

Diversity of clonal architecture is a common key feature among a broad range of malignancies, and it has been addressed from different perspectives [1–9]. It has been more than 40 years since the concept of clonal evolution in cancer was first proposed [10]; however, many questions about clonality are still unanswered. Recently, the quantitative nature of next-generation sequencing data has allowed for investigating genetic diversity among tumors and elucidating the clonal architecture of cancers with higher resolution [4,11]. Determining the profiles of somatic point mutations and copy number alterations (CNAs) of specific subpopulations in a tumor that exhibits intratumor heterogeneity (ITH) remains as one of the challenging issues in the field [7,12–15].

Clonal heterogeneity within malignancies has been implicated as a driving force of tumor development and progression because a high degree of genetic variability is associated with an increased risk of subclones having a proliferative advantage, thus leading to clonal expansion [16]. The clonal structures of several cancers have been described as widely diverse patterns ranging from simple monoclonal to complex polyclonal structures [17–19]. At the molecular level, clonal genetic diversity seems to be associated with more aggressive disease [20]. However, the association of the levels of ITH with disease outcome and with efficacy of therapeutic intervention depends on the type of malignancy. For example, in chronic lymphocytic leukemia, subclonal mutations are associated with unfavorable outcomes [21]; however, glioblastoma patients with subclonal mutations manifested longer event-free survival than patients with clonal tumors [22]. Thus, achieving a better understanding of the clonal structure of cancer cells is of vital importance for prognostics and targeted therapies [22]. Widely diverse clonal architecture for each patient's tumor indicates a variation in mutational evolution, and thus knowledge about the clonal architecture is crucial for optimizing a patient's treatment [16,17,23,24]. Recently the number, size, and mutational content of clones within a patient's tumor have been explored extensively [5,13,21,23,25–27].

Adult T-cell leukemia/lymphoma (ATL) is an aggressive and complex malignancy that is caused by infection with human T-cell leukemia virus type-1 (HTLV-1) over a long latency period [28–33]. An analysis of the clonality pattern and the number of clones based on the provirus integration sites [34] indicates that the absolute abundance of infected and leukemic clones is a determining factor for ATL development [35,36]. High-throughput longitudinal analysis indicates that infected individuals with small clones and polyclonal patterns remain healthy over time, whereas those with large clones having an oligo- or monoclonal pattern develop ATL [37,38]. Also, recently a study on multi-organ clonality analysis in Simian T-Lymphotropic Virus type-1 associated leukemia- a simian counterpart of ATL- reported a complex clonality pattern in this disease [39]. However, the molecular mechanism and pathogenesis behind clonal expansion in ATL remain largely unknown, and the clonal composition based on somatic mutations in ATL has not been monitored.

Although most of the studies analyzing genetic abnormalities of ATL have focused on a limited number of candidate genes [40], a recent study comprehensively revealed the genome-wide mutational spectrum of a large number of ATL cases and proposed a list of frequently mutated genes in ATL [41]. To our knowledge, clonality analysis based on tumor mutational diversity has never been investigated in ATL because it requires costly and complex analysis and needs deep multidisciplinary knowledge for data interpretation. ITH in ATL has the potential to be used as a prognostic biomarker as well as a measure for disease pathogenesis and therapeutic response. Thus, the main aim of the current study was to address clonal heterogeneity in ATL based on mutation profiles of cross-sectional whole-exome sequencing (WES) samples.

Methods

ATL Samples

We used 71 samples from different subtypes of ATL (smoldering, $N = 5$; chronic, $N = 22$; acute, $N = 33$; and lymphoma, $N = 11$) and 71 non-tumor DNA from the same patient deposited in the European Genome-phenome Archive (EGA) with accession number EGAD00001001410 [41]. Sequencing libraries were prepared from tumor DNA (peripheral blood mononuclear cells -PBMCs-) and non-tumor DNA (buccal mucosa) from the same patient to identify acquired (somatic) mutations. The information regarding the samples is included in Table S1.

SNV Bioinformatics Pipeline

We analyzed single-nucleotide variants (SNVs) using our bioinformatics pipeline described below and in Figure S1. In brief, raw sequencing data underwent the following steps: alignment, sorting, indexing, PCR duplicate removal, variant calling, report generation, and data visualization. The short sequencing reads were aligned to the human genome sequence hg38 [42] using the Burrows-Wheeler Aligner (BWA) [43]. Sorting, indexing, and removal of PCR duplicates were conducted with Samtools [44]. SNV detection was performed with the Genome Analysis Toolkit (GATK) HaplotypeCaller [45]. Population variants were removed using dbSNP for human sequences (Version 142) [46]. Further analysis and variant classification were conducted by our in-house Perl and Python scripts. Finally, detected SNVs were annotated by ANNOVAR [47]. The processing of tumor/normal pairs was carried out under identical conditions, and variants detected within the normal matched control samples were removed from tumor variants to retrieve only somatic mutations. In this manuscript, we limited our analysis to mutations with a depth of ≥10 supporting tags.

CNA Bioinformatics Pipeline

Somatic CNAs were detected using data from matched tumor–normal pairs. Exome sequencing reads were aligned against the human reference genome (hg38) using BWA [43]. Subsequently, Samtools [44] mpileup files were used as an input for Varscan v2.2.4 [48]. Segmentation was performed using the DNAcopy library from BioConductor [49]. Gistic2 was used for final analysis and visualization [50]. We analyzed CNAs using our bioinformatics pipeline described in Figure S1.

Inference of Genetic ITH Using SciClone

SciClone [51] was used as an approach to infer the clonal composition of each tumor sample. The output consisting of CNAs and SNVs detected within coding regions was used as input for SciClone. Clonal analysis was performed with a > 10% variant allele frequency (VAF) threshold using a variational Bayesian mixture model implemented by SciClone.

Results

To understand the patterns of somatic mutations in ATL, we characterized genome aberrations from 71 patients with different subtypes of ATL. We used the bioinformatics tool SciClone to quantify ITH from exome-sequencing data of tumor and matched normal samples.

Landscape of Genetic Alterations in ATL

We identified an average of 697 SNVs in coding regions from each sample using our SNV analysis pipeline (Figure S1). A comprehensive list of detected mutations with information including the type of mutation, VAF, and corresponding annotations for each sample is provided in Table S2. The relative abundance of the detected mutation categories including nonsynonymous, synonymous, stop gain, stop loss, frameshift deletion, and frameshift insertion in each sample and across all samples is presented in Figure 1. The total point mutation content in coding regions in genomic DNA from individual tumors ranged from 313 to 2365. The distribution of the somatic mutations varied in a continuous manner among the samples (Figure 2*A*). The number of SNVs detected in aggressive ATL (acute and lymphoma subtypes) was slightly higher than ATL samples consisting of indolent subtypes (chronic and smoldering) but was not statistically significant (*P*-value, 0.72; Figure S2).

We also performed copy number analysis using WES data via the CNA bioinformatics pipeline shown in Figure S1. The percentages of regions with copy number profiles of neutral, amplifications, deletions, and homozygous deletions in each sample and across all samples are presented in Figure S3a. The numbers were retrieved from outputs of Varscan2, of which $\log_2$ ratios of changes in copy number for the analyzed regions of <–0.25 and> 0.25 were considered as deletions and amplifications, respectively. Of the analyzed regions, 30%, 38%, 31%, and 1% were amplifications, neutral, deletions, and homozygous deletions, respectively (Figure S3b). Figure 2*A* represents the total number of events detected during copy number analysis.

After the copy number analysis, we distinguished the SNVs located within regions with neutral copy numbers from those located within regions with altered copy numbers (amplifications and deletions). Approximately 80% of detected coding SNVs were located in regions with a neutral copy number (Figure 2*B* and Table S1). We used these regions to analyze the ITH in each sample. The distributions of the somatic mutations in these regions across samples and within each subtype are presented in Figures 2*B* and S2. Samples with aggressive ATL had more SNVs located in copy number altered regions (P = .049) (Figure S3).

We also analyzed significantly altered regions of amplification and deletion across the samples (Figure 3). Information regarding cytoband, q-value, wide-peak boundaries, and genes in wide peaks is presented in Table S3.

Regions with significant changes to the copy number were detected in most tumors. Significant loss of 1p13.1, in which *CD58* is located, was observed (q = 0.000012641). Significant loss of 9p21.3, in which *CDKN2A* and *CDKN2B* are located, was observed (q = 0.000030436). Significant loss of 10p14, in which *GATA3* is located, was observed (q = 0.0055013). Significant loss of 17p13.1, in which *CD68* and *TP53* are located, was observed (q = 0.012124). Loss in the 6p21.33 region, the chromosomal location of *HLA-B*, was also observed (q = 0.0386). Significant gain was observed in 9p24.1, the chromosomal location of *CD274*, which is commonly referred to as *PDL1* (q = 0.0000024788). Significant gain was observed in 6p25.3, the chromosomal location of *IRF4* (q = 0.034469). Significant gain was observed in 14q32.2, the chromosomal location of *SETD3* (q = 0.00046686; Figure 3).

Detecting Intratumor Genetic Heterogeneity by SciClone

Clustering of mutations revealed the subclonal structure of ATL in patients harboring multiple mutations. We used the detected SNV and CNA profiles for each sample to analyze the corresponding clonal/subclonal architecture using SciClone. To minimize the effect of CNAs and regions with loss of heterozygosity, we considered SNVs in neutral copy number regions. The results of four representative samples from smoldering, chronic, acute, and lymphoma subtypes of ATL are shown in Figure 4. The visualized outputs across the remaining samples including SNVs both in neutral and altered copy number regions are presented in Figure S6.

Subclonal Mutations Identified Within Each Sample

To provide further information on subclonal architecture based on mutational profiles, we used a list of recently identified highly

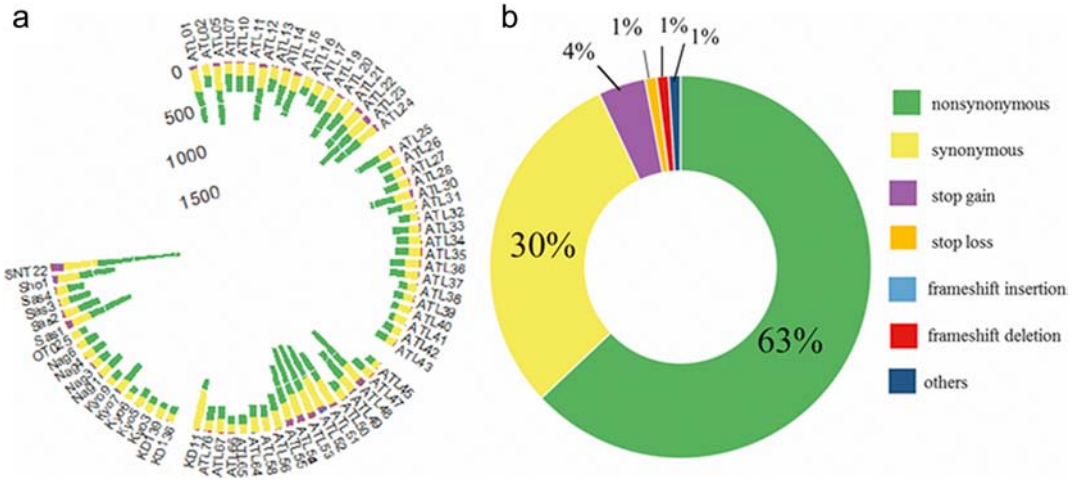

Figure 1. Somatic SNV profiles. (a) Distribution of different types of mutations within coding regions among samples. The proportion of nonsynonymous, synonymous, stop gain, stop loss, frameshift insertion, and frameshift deletion mutations is indicated. (b) Relative abundance of the detected mutation categories across samples. The color legend corresponds to both 1a and 1b.

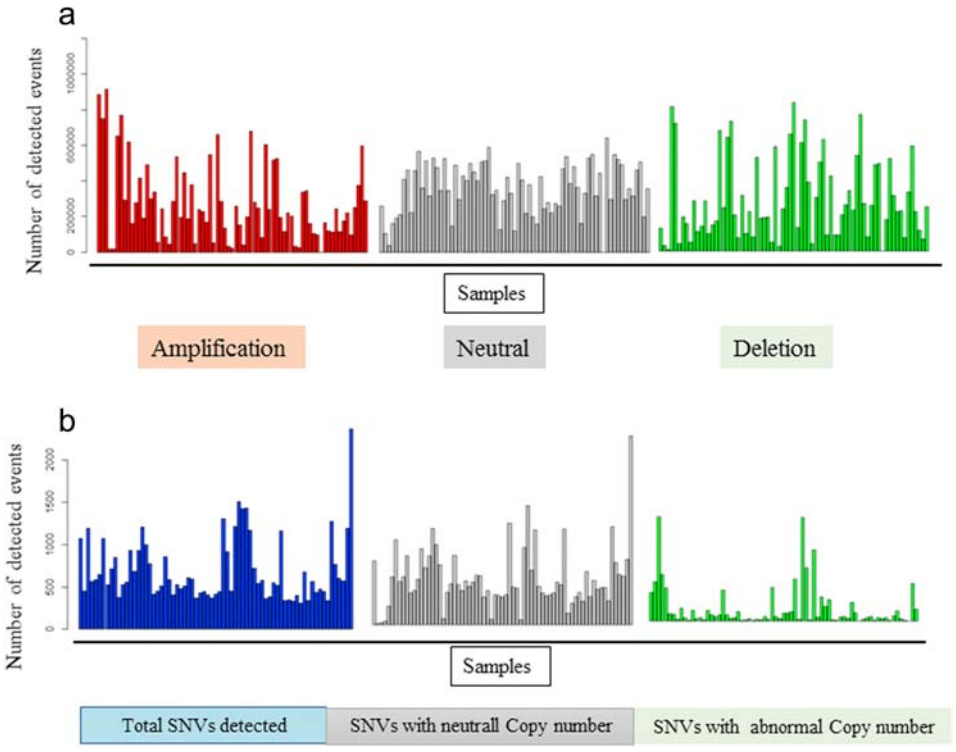

Figure 2. Mutations in regions of copy number neutral, amplification and deletion among all samples. a) Somatic copy number analysis across samples. Numbers of detected amplification, neutral, and deletion events detected from each sample following copy number analysis are presented. b) Total detected somatic SNVs, SNVs located in regions with a neutral copy number, and SNVs located in regions with an altered copy number. The order of samples is identical to that shown in Figure 1*A*.

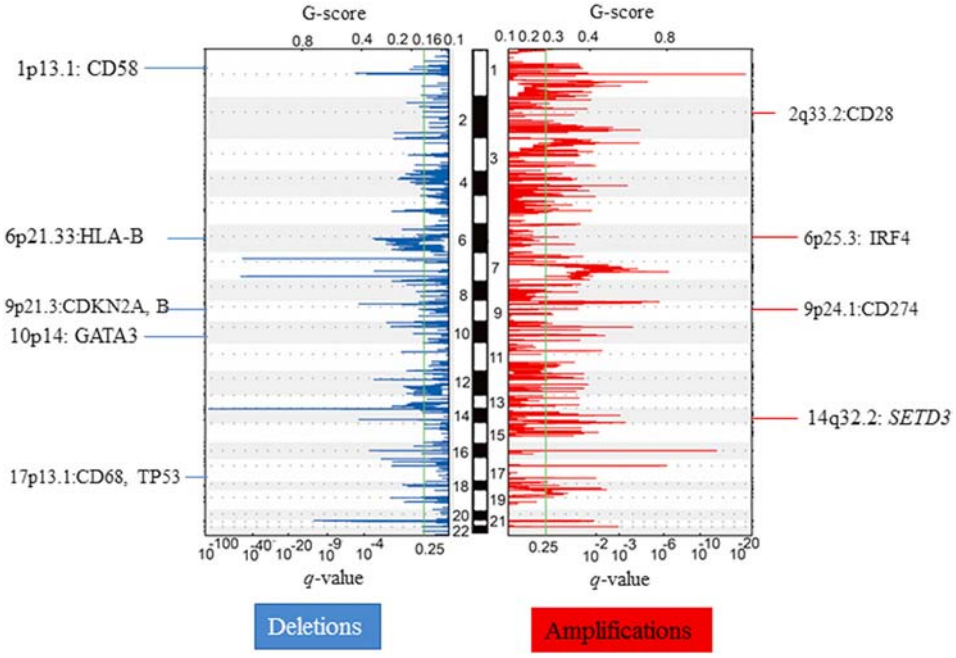

Figure 3. CNA in specific regions detected by GISTIC 2.0. Significantly observed CNAs across samples are presented. The genome is oriented vertically from top to bottom along the *y* axis. Numbers in the middle refer to the chromosome number. GISTIC *q*-values indicating the false discovery rate at each locus are presented on a log scale (*x* axis). Annotated peaks have residual q < 0.25. Red bars (right side), blue bars (left side) indicate amplifications and deletions, respectively. For each plot, known or interesting (i.e., with possible biological impact in ATL) candidate genes are written in black.

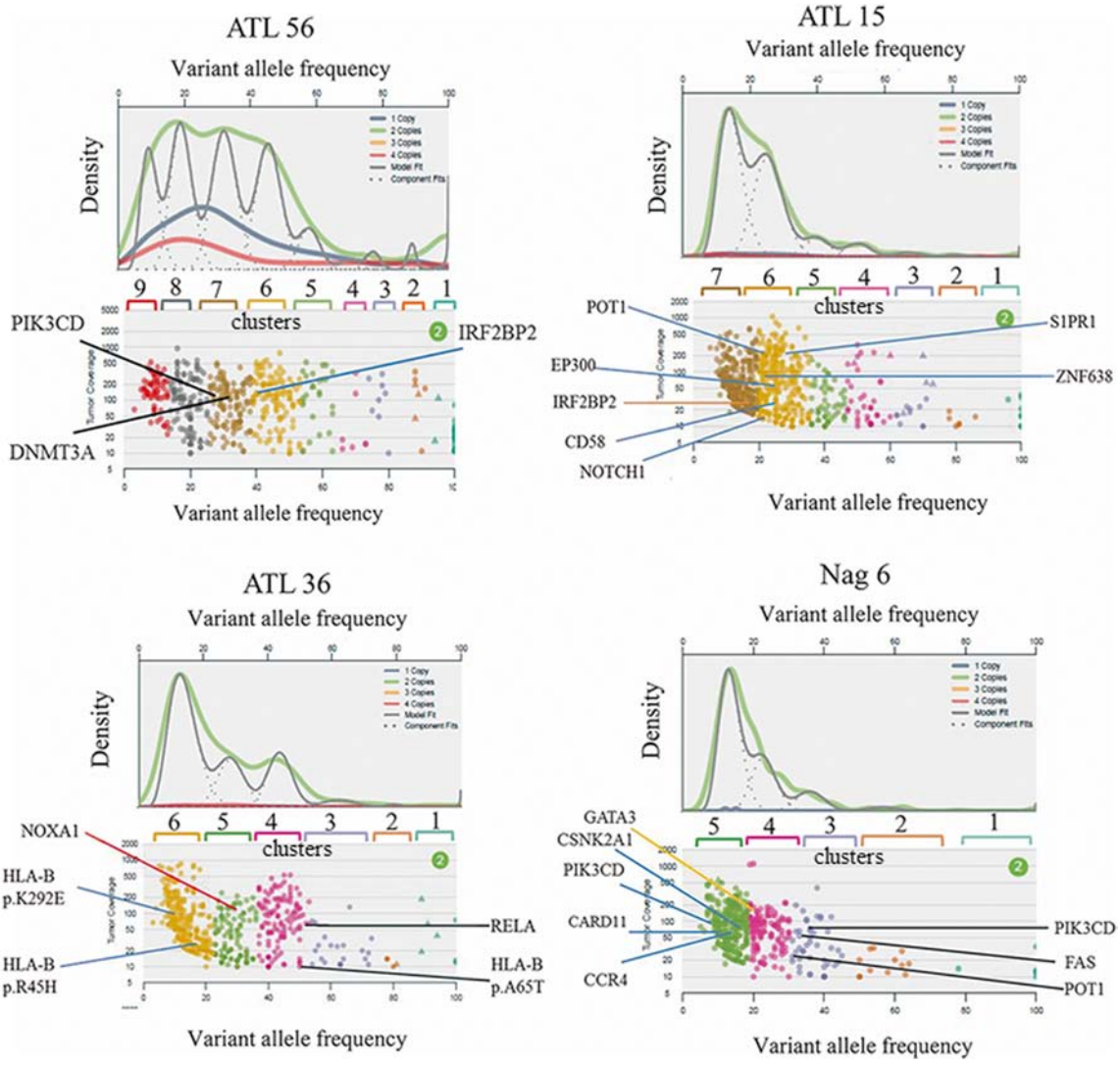

Figure 4. Significantly mutated genes and mutational clonal architecture among 71 ATL samples. VAF is plotted against density among neutral copy number variants, and VAF is plotted against tumor coverage (depth) for four representative samples from different subtypes (smoldering, chronic, acute, and lymphoma). (a) Kernel density plots of VAFs across neutral copy number regions. (b–d) VAFs plotted versus read depth for each sample. The output of SciClone for neutral copy number regions is presented along with significant genes in each sample. Points of the same color belong to the same cluster. Clusters are numbered from right to left (i.e., from higher to lower VAFs). ATL56, ATL15, ATL36, and Nag6 had nine, seven, six, and five clusters, respectively. Significantly mutated genes in ATL are marked for each cluster.

mutated genes in ATL [40] and analyzed the clonal/subclonal status of these genes in each sample (Figures 4, S6 and Table S4). Subclones are numbered based on their descending order of VAF. The last subclone is the cluster with the lowest VAF.

To further explain the observed results and their interpretation, we present four main samples. ATL56 is derived from a patient with lymphoma type ATL with 132.7% proviral load (PVL), a measure of the number of provirus copies among 100 peripheral blood mononuclear cells. We detected 722 total coding SNVs, with 458 SNVs in neutral copy number regions and 264 SNVs in altered copy number regions. SciClone detected nine clusters in this case. Mutations in *FAS*, *NOTCH1*, and *TP53* were located in a region with an altered copy number (i.e., one copy). *DNMT3A* and *PIK3CD* mutations were clustered together in subclone-7. Mutation of *IRF2BP2* was clustered in subclone-6 (Figure 4).

ATL15 is derived from an acute patient with 84.9% PVL. We detected 850 total coding SNVs, with 813 SNVs in neutral copy number regions and 37 SNVs in regions with an altered copy number. SciClone detected seven clusters in this case. We also examined the overlap of mutated genes in this sample with the list of genes that are significantly mutated in ATL. The clonal status of the overlapping genes is indicated in Figure 4. Mutation of *TP53* occurred in a region with an altered copy number (Figure S6). An *IRF2BP2* mutation was clustered in subclone-7, which had the lowest VAF. Of note, *CD58*, *EP300*, *NOTCH1*, *POT1*, *S1PR1*, and *ZNF638* mutations were clustered together in subclone-6 (Figure 4).

ATL36 is derived from a chronic patient with 78.6% PVL. We detected 609 total coding SNVs, with 591 SNVs in neutral copy number regions and 18 SNVs in regions with an altered copy number. SciClone detected six clusters in this case. *HLA-B*, *NOXA1*,

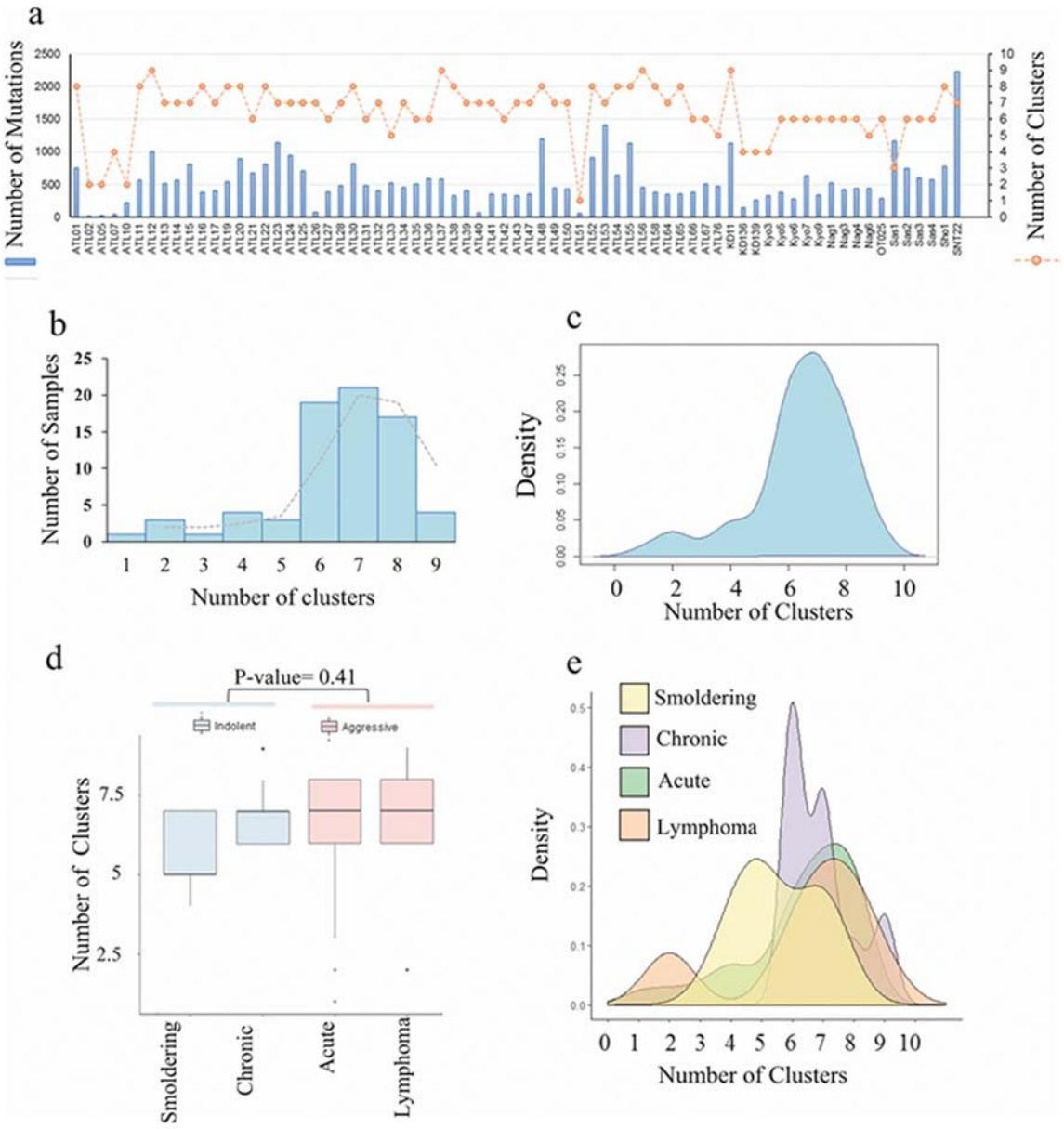

Figure 5. Distribution of mutational clusters in ATL. a) The number of coding mutations used for clustering in each sample and the number of clusters detected across all samples. Blue bars represent the number of mutations in each sample. Orange dots represent the number of clusters. b) Distribution and kernel density (gray line) of the number of clusters across the 71 ATL samples. c) Kernel density showing the number of clusters. d) The number of clusters in each subtype of ATL. e) Kernel density of clusters in each ATL subtype (smoldering, chronic, acute, and lymphoma).

and *RELA* were the mutated genes that overlapped with the list of significantly mutated genes in ATL. Mutations in *HLA-B* were in three different locations. Nonsynonymous mutations of *HLA-B* with p.K292E in exon 4 and p.R45H in exon 2 were clustered together in subclone-6, which had the lowest VAF. *HLA-B* with p.A65T in exon 2 and the *RELA* mutation were clustered in subclone-4. *NOXA1* showed a stop gain mutation and was clustered in subclone-5 (Figure 4).

Nag6 is derived from a smoldering patient with 34.88% PVL. We detected 441 total coding SNVs, with 439 SNVs in neutral copy number regions and 2 SNVs in regions with an altered copy number. SciClone detected five clusters in this case. Mutations in *PIK3CD*, *FAS*, and *POT1* were clustered in subclone-3. The *GATA3* mutation was clustered in subclone-4. Mutations in *PRKCB*, *CSNK2A1*, *CCR4*, and *CARD11* were clustered in subclone-5, which had the lowest VAF (Figure 4).

We describe below the findings from five aggressive samples (lymphoma and acute ATL) that harbored mutations and clusters of interest. Additional samples are included in Figure S6.

Sas1 is derived from an acute patient with 84.6% PVL. We detected 1273 total coding SNVs, with 1163 SNVs in neutral copy number regions and 110 SNVs in regions with an altered copy number. SciClone detected three clusters in this case. *S1PR1* (p.M80I), an *IRF2BP2* mutation, and *HLA-B* (p.V272 M) were clustered in subclone-3, which had the lowest VAF, whereas *S1PR1*:stop gain, *PRKCB*, *TP53*, *CCR4*, *RHOA*, *HLA-B* (p.G338R), *HLA-B* (p.Y140F), and *NOTCH1* were clustered in subclone-2 (Figure S6).

ATL50 is derived from an acute patient with 107.1% PVL. We detected 451 total coding SNVs, with 433 SNVs in neutral copy number regions and 18 SNVs in regions with an altered copy number. SciClone detected seven clusters in this case. Mutation of *HLA-B* (p.D98Y) was clustered in the main clone with the highest VAF, indicating that it is shared among almost all cells of the population and evolved during a very early stage of clonal evolution. Mutations in *IRF2BP2*, *IRF4*, *PLCG1*, and *HLA-B* (p.E69G) were clustered in subclone-5. Mutations in *HLA-B* (p.A93T) and *HLA-B* (p.R45H) were clustered in subclone-6. Mutations in *HLA-B* (p.R243W) and *HLA-B* (p.D201E) were clustered in subclone-7, which had the lowest VAF (Figure S6).

ATL51 is derived from a patient with acute type ATL with 34.6% PVL. We detected 1214 total coding SNVs, with 59 SNVs in neutral copy number regions and 1155 SNVs (a particularly high number) in altered copy number regions. SciClone detected only one cluster in this case. A mutation in *HLA-B* was highly abundant and was detected in more than nine regions. Mutations in *HLA-B*, *ATXN1*, *STAT3*, and *IKBKB* were detected in regions with an altered copy number (three copies; Figure S6).

Kyo5 is derived from a patient with acute type ATL with 87.38% PVL. We detected 397 total coding SNVs, with 381 SNVs in neutral copy number regions and 16 SNVs in altered copy number regions. SciClone detected six clusters in this case. Multiple mutations in *HLA-B* (at five positions) were also detected in this patient. All *HLA-B* mutations were clustered together in subclone-6, which had the lowest VAF. Two mutations in *CARD11* at p.S622Y and p.S622P were clustered in subclone-5. A mutation in *GATA3* was also clustered in subclone-5. A mutation in *TP53* was clustered in subclone-4. A mutation in *CBLB* was clustered in subclone-3. A mutation of *PRKCB* was clustered in subclone-2 (Figure S6).

ATL01 is derived from a patient with lymphoma type ATL with 25.8% PVL. We detected 1074 total coding SNVs, with 756 SNVs in neutral copy number regions and 318 SNVs in regions with an altered copy number. SciClone detected eight clusters in this case. Mutations in *HLA-B* (p.V9L), *NOTCH1* (p.T349P), and *TP53* were clustered in subclone-6. Mutations in *ZFP36L2* (p.G471D), *ZFP36L2* (p.R188H), and *NOTCH1* (stop gain) were clustered in subclone-7. Mutations in *HLA-B* (stop gain), *HLA-B* (p.G338S), and *HLA-B* (p.Y140F) were clustered in subclone-8, which had the lowest VAF. (Figure S6).

The distribution of isolated mutations and detected clusters across all samples and among different subtypes is summarized in Figure 5*A*. The number of clusters ranged from one to nine, with an average of six clusters across the samples (the median estimated number of clusters was seven). Figure 5, *B* and *C* illustrate the distribution of clusters across all samples. Although the number of clonal/subclonal frequency modes tended to increase slightly with the number of mutations, the relationship was not linear (R^2 = 0.1718; Figure S4). Two or more clusters were observed to coexist in >94% of the samples. Therefore, we concluded that genetic ITH occurs in the majority of ATL samples in this study. To determine whether indolent and aggressive ATL differ in their clonality, we compared the distribution of clones, in both a case-by-case and an overall distribution manner, and noted that aggressive ATL was likely to result in slightly more clonal clusters than did indolent types, although this difference was not significant (P = .41; Figure 5*D*). These distributions suggest that during the early stages of disease in indolent ATL, patients already display a wide variety of clonal clusters, which thus indicates the presence of mutational evolution. The distribution of clonal clusters among different subtypes of ATL is shown by boxplots and kernel density plots in Figure 5, *D* and *E*. Analysis of the mutation and clinical data among different subtypes of ATL showed that patients with the acute form had averages of 96% PVL, 4.6 clusters, and 734 coding mutations and were an average of 66 years old. These averages for lymphoma patients were 97% PVL, 6.2 clusters, 638 coding mutations, and 66 years old; for chronic patients, they were 80% PVL, 5.2 clusters, 644 coding mutations, and 65 years old; and for smoldering patients, they were 27% PVL, 4.5 clusters, 831 coding mutations, and 58 years old.

HLA-B was one of the highly mutated genes, with an average VAF of 25.96 (range, 7–100; median, 19). In most samples in this study, *HLA-B* harbored non-synonymous mutations in more than one region. *HLA-B* mutations were typically clustered in subclones with low VAF. *CARD11* was one of the frequently mutated genes, with an average VAF of 25.65 (range, 10–74; median, 24). *CARD11* mutations were typically clustered in subclones with low VAF. ATL13, Kyo5, and ATL55 had multiple *CARD11* mutations. In ATL13, the three mutations p.S433R, p.E626K, and p.S621F were clustered separately in subclones-5, –6, and– 7, respectively. In Kyo5, mutations p.S622Y and p.S622P were clustered in subclone-5. In ATL55, both mutations were clustered in subclone-8, which had the lowest VAF. *NOTCH1* was one of the frequently mutated genes, with an average VAF of 20.9 (range, 2–38; median, 21). This mutation was typically observed in subclones with low VAF. Sas1 and Sas2 had multiple *NOTCH1* mutations. In Sas1, two mutations (p.T349P and p.G200 V) were clustered in subclone-2. In Sas2, three mutations (p.V1216 L, p.T349P, and p.A348P) were clustered in subclone-6, which had the lowest VAF. *CCR4* was one of the frequently mutated genes, with an average VAF of 40.76 (range, 14–81; median, 44). This mutation was almost always observed in subclones with moderate VAF. Most of the samples contained only a single *CCR4* mutation; however, ATL10 had two *CCR4* mutations in p.Y331X (stop gain) and p.G33D (non-synonymous), both of which were clustered in the clone with the highest VAF. Nag6, ATL55, ATL33, and ATL13 each had a *CCR4* mutation in the subclone with the lowest VAF. *TP53* was one of the frequently mutated genes, with average VAF of 42.4 (range, 14–86; median, 37). This mutation was typically observed in subclones with moderate VAF. Kyo9 was the only sample that had two mutations of *TP53* at p.S246P and p.T245P, both of which were clustered in subclone-6, which had the lowest VAF. In other samples with a *TP53* mutation, this mutation was found in subclones with moderate VAF. *IRF4* was one of the frequently mutated genes, with an average VAF of 36.33 (range, 11–50; median, 42). This mutation was almost exclusively observed in subclones with moderate VAF. *PLCG1* was one of the frequently mutated genes, with an average VAF of 32.94 (range, 10–72; median, 42). This mutation was almost always observed in subclones with moderate VAF. ATL27 had three mutations of *PLCG1* at p.R48W, p.S866R, and p.V850A, which were found in subclone-1, subclone-2, and subclone-4, respectively (Figure S5).

Discussion

Clonal heterogeneity plays a central role in cancer, and quantification of ITH is an essential measure of tumor evolution [13]. Clonal heterogeneity complicates our understanding of tumor biology; in-depth characterization of ITH is needed for improvement of therapeutic responses and personalized medicine [52]. Genomic

instability and ITH have the potential to be useful prognostic and predictive measures in malignancies including ATL. Clonal genetic diversity in tumors negatively affects the clinical outcomes. Thus, recent studies have emphasized the significance of quantifying ITH and have detected and monitored the dynamics of subclonal events within tumors [20,53]. In this study, we tried to improve our understanding of tumor heterogeneity and analyze its correlation with different stages of disease in ATL to open new paths for its contribution to personalized medicine.

Combining ITH data with clinical information in a simple, quantitative, and practical manner is useful for clinical decision-making. However, it is difficult to overcome the technical hurdles in analyzing SNVs and CNAs and to use the appropriate bioinformatic pipeline for clustering the detected mutations. To overcome these difficulties, we performed an analysis of ITH in 71 ATL patients using 142 WES data for tumors and matched normal samples. Remarkably, the results showed a wide range of modes over clonal frequencies, with only one case showing a single cluster, and 94% of cases having more than two clusters. These findings indicate the presence of an extensive intratumor subclonal diversity in ATL.

During the past several years, the presence of considerable ITH in hematological malignancies and cancers, including cancers of the ovary, breast, lung, prostate, pancreas, bladder, and kidney, has been reported [21,54–57]. These studies have contributed substantially to a greater understanding of ITH and have suggested the potential application of ITH itself as a biomarker for prognosis [57,58]. More extensive studies are, however, needed to draw definitive conclusions about the role of ITH in the initiation, maintenance, and progression of cancers, as well as its clinical implications. Compared with other malignancies, ATL has been relatively neglected, and even the landscape of genomic events in ATL has been revealed only recently [41]. The current study is the first attempt to investigate the role of ITH in ATL. Clearly, more works needs to be conducted on ITH in ATL using various multiregional and/or longitudinal datasets.

As in other types of cancers, ITH is likely to be of potential biological and clinical significance in ATL. Considering the significant association between a high clone number and the poor outcome reported in several malignancies, the detection of a large number of clusters in these ATL samples is consistent with the fact that most ATL patients manifest very poor prognoses and therapeutic outcomes [31,33,59]. Overall, we observed a relatively large number of mutations in these subclones. We also noted the presence of a large number of small clones among these samples. Small clone sizes indicate their late evolution during tumor progression. The coexistence of multiple subclones indicates their similar fitness advantage, which prevents them from outgrowing each other. Therefore, we can hypothesize that mutational evolution is recently active and continuing in these ATL cases.

Recently, a high-throughput study of the mutation profiles of ATL patients proposed a list of mutated genes of particular relevance [41]; however, the clinical relevance of these mutated genes has not yet been clearly demonstrated. They also comprehensively analyzed viral gene expression (including HBZ and Tax). They reported that HBZ are generally detectable in all ATL cases, but Tax expression is rare [41]. Our data presented here are consistent with those from the previous publication by [41]. We also analyzed the clonal distribution of the top 50 mutated genes in ATL for each sample in this study. Alteration of cell cycle–related genes such as *TP53* and *CDKN2A* has been suggested as a determining factor for acute transformation in ATL cases [40]. *TP53* has been reported as a candidate gene that plays important roles in acute transformation [60]. Mutation of *TP53* was considered a driving force for clonal expansion. In our analysis, we confirmed the presence of *TP53* in subclones with relatively moderate or high VAF. *CDKN2A* has been suggested as a probable candidate tumor suppressor gene in ATL [40]. Loss of *CDKN2A* in acute ATL may lead to cell cycle deregulation [61]. We also confirmed the loss of *CDKN2A* in our cases. Moreover, genomic alteration of *CD58*, which plays a role in escape from immunosurveillance, was reported in acute ATL [40]. It has been reported that using immunosuppressive therapy for HTLV-1 carriers leads to early development of ATL [62–64]. Thus, the presence of genomic alterations related to immune escape, such as *CD58* mutation, might be one of the significant determining factors that need to be considered in developing immunotherapeutic approaches for ATL. In addition, mutation of *CCR4* is an important determinant of the clinical course of ATL, and a frameshift mutation in this gene has been linked to poor prognosis [65]. *CCR4* is expressed on the surface of 90% of ATL cells [66], and a monoclonal antibody against *CCR4* (mogamulizumab) demonstrated very strong cytotoxicity against ATL cells [67,68]. *CCR4* mutations in our study were clustered in subclones with medium and low VAFs. The effect of harboring a *CCR4* mutation and its clonal status on the response to mogamulizumab treatment is a topic that should be investigated in future studies.

Longitudinal monitoring of clonality among infected cells using HTLV-1 integration sites indicates that clonal expansion of infected cells occurs from the early stages of infection, even when individuals are still healthy and are diagnosed as asymptomatic carriers. Individuals with a largely expanded infected clone have a high risk of ATL development [37,38]. However, it is not clear whether the expanded cell populations are homogeneous or heterogeneous at a mutation level. In this study, analyzing smoldering, chronic, acute, and lymphoma subtypes of ATL, suggested that expanded cells are not homogeneous. A high degree of ITH was evident in the analyzed cases of this study, even among patients with smoldering and chronic subtypes, which represent early stages of the disease. Therefore, we suggest that, like other malignancies, the presence of heterogeneity among clones (ITH) is likely to be an essential factor for ATL development. Also, ITH is likely to occur during early stages of ATL development. Indeed, the presence of more than one clone in many tumor types raises important—and thus far unanswered—questions regarding the biological mechanisms behind ITH. Why is heterogeneity present among various tumor types, and why does the fittest clone not take over within a tumor? In pursuit of revealing the functional relevance of ITH, a highly interesting concept of clonal cooperation has been suggested. In the case of breast cancer, an analysis of the tumorigenicity of different clones using in vivo models showed the coexistence of two types of clones that are essential for tumorigenicity [69,70]. It has been suggested that different clones, including those that are most fit, have a paracrine interdependence with other subclones, and hence clonal cooperation is essential for maintaining tumorigenicity [69,70]. Further in-depth functional analyses of ITH in various malignancies are required to clarify the significant role of ITH in cancer development.

Conclusion

Our findings suggest that clonal diversity might provide additional prognostic information for ATL. Measurement of ITH might thus

eventually become an aid to clinical decision-making with respect to treatment of patients with ATL. Although these observations require confirmation by longitudinal analyses of ATL cases pre- and post-chemotherapy as well as molecular target therapy, clonal heterogeneity might hold promise for a deeper understanding of ATL. As we move toward an era of personalized medicine for ATL and other cancers, we need to build an understanding of the clinical impact of subclone admixtures containing specific mutations. In the case of ATL, the presence of multiple subclones may increase the clonal competition, and thus the probability of the presence of resistant clones among a complex population of subclones is very high.

Declarations

Ethics Approval

Access to the raw sequencing data was approved based on the agreement between Kyoto University and The University of Tokyo.

Availability of Data and Material

The raw sequencing data have been deposited in European Genome-phenome Archive(EGA) under accession number of EGAD00001001410.

Disclosure

The authors have declared no conflicts of interest.

Funding

This work was supported by a "Kakenhi" grant from the Japan Society for the Promotion of Science [grant number 17 K15044]; and The Tokyo Biochemical Research Foundation [TBRF-RF 17–104]; and Japan Agency for Medical Research and Development [ck0106256h0001].

Authors' Contributions

AF and SF contributed to the conception and design of the study, development of the methodology, analysis and interpretation of the data (e.g., statistical analysis and computational analysis), and the writing of the first draft of the manuscript, as well as designing the figures. RK and WM contributed in bioinformatics and methodology. KN provided administrative support. TW, AU and MI contributed to the medical and biological interpretation of the data.TW, RK and WM assisted with critical revision of the manuscript. All authors read and approved the final manuscript.

Acknowledgements

We are grateful to professor Seishi Ogawa from Kyoto University for providing raw sequencing data.

AF expresses deep respect and gratitude to the Otsuka Toshimi scholarship foundation for supporting his graduate studies and to U. Firouzi for help in the design of figures.

Computational analyses were provided by the Supercomputer System at Human Genome Center, The Institute of Medical Science, The University of Tokyo. We appreciate the technical assistance of H. Nishijima.

Appendix A. Supplementary Data

Supplementary data to this article can be found online at https://doi.org/10.1016/j.neo.2018.07.001.

References

[1] Greaves M (2015). Evolutionary determinants of cancer. *Cancer Discov* **5**(8), 806–820.

[2] Sprouffske K, Merlo LM, Gerrish PJ, Maley CC, and Sniegowski PD (2012). Cancer in light of experimental evolution. *Curr Biol* **22**(17), R762-771.

[3] Merlo LMF, Pepper JW, Reid BJ, and Maley CC (2006). Cancer as an evolutionary and ecological process. *Nat Rev Cancer* **6**(12), 924–935.

[4] Nik-Zainal S, Van Loo P, Wedge DC, Alexandrov LB, Greenman CD, Lau KW, Raine K, Jones D, Marshall J, and Ramakrishna M, et al (2012). The life history of 21 breast cancers. *Cell* **149**(5), 994–1007.

[5] Ding L, Ley TJ, Larson DE, Miller CA, Koboldt DC, Welch JS, Ritchey JK, Young MA, Lamprecht T, and McLellan MD, et al (2012). Clonal evolution in relapsed acute myeloid leukaemia revealed by whole-genome sequencing. *Nature* **481**(7382), 506–510.

[6] Makishima H, Yoshizato T, Yoshida K, Sekeres MA, Radivoyevitch T, Suzuki H, Przychodzen B, Nagata Y, Meggendorfer M, and Sanada M, et al (2017). Dynamics of clonal evolution in myelodysplastic syndromes. *Nat Genet* **49**(2), 204–212.

[7] Shah SP, Roth A, Goya R, Oloumi A, Ha G, Zhao Y, Turashvili G, Ding J, Tse K, and Haffari G, et al (2012). The clonal and mutational evolution spectrum of primary triple-negative breast cancers. *Nature* **486**(7403), 395–399.

[8] Roth A, McPherson A, Laks E, Biele J, Yap D, Wan A, Smith MA, Nielsen CB, McAlpine JN, and Aparicio S, et al (2016). Clonal genotype and population structure inference from single-cell tumor sequencing. *Nat Methods* **13**(7), 573–576.

[9] Wang Y, Waters J, Leung ML, Unruh A, Roh W, Shi X, Chen K, Scheet P, Vattathil S, and Liang H, et al (2014). Clonal evolution in breast cancer revealed by single nucleus genome sequencing. *Nature* **512**(7513), 155–160.

[10] Nowell PC (1976). The clonal evolution of tumor cell populations. *Science* **194**(4260), 23–28.

[11] Kroigard AB, Larsen MJ, Laenkholm AV, Knoop AS, Jensen JD, Bak M, Mollenhauer J, Kruse TA, and Thomassen M (2015). Clonal expansion and linear genome evolution through breast cancer progression from pre-invasive stages to asynchronous metastasis. *Oncotarget* **6**(8), 5634–5649.

[12] Sottoriva A, Kang H, Ma Z, Graham TA, Salomon MP, Zhao J, Marjoram P, Siegmund K, Press MF, and Shibata D, et al (2015). A Big Bang model of human colorectal tumor growth. *Nat Genet* **47**(3), 209–216.

[13] Andor N, Graham TA, Jansen M, Xia LC, Aktipis CA, Petritsch C, Ji HP, and Maley CC (2016). Pan-cancer analysis of the extent and consequences of intratumor heterogeneity. *Nat Med* **22**(1), 105–113.

[14] Hardiman KM, Ulintz PJ, Kuick RD, Hovelson DH, Gates CM, Bhasi A, Rodrigues Grant A, Liu J, Cani AK, and Greenson JK, et al (2016). Intra-tumor genetic heterogeneity in rectal cancer. *Lab Invest* **96**(1), 4–15.

[15] Fischer A, Vazquez-Garcia I, Illingworth CJR, and Mustonen V (2014). High-definition reconstruction of clonal composition in cancer. *Cell Rep* **7**(5), 1740–1752.

[16] McGranahan N, Favero F, de Bruin EC, Birkbak NJ, Szallasi Z, and Swanton C (2015). Clonal status of actionable driver events and the timing of mutational processes in cancer evolution. *Sci Transl Med* **7**(283), 1–11. doi:10.1126/scitranslmed.aaa1408 283ra254.

[17] Kandoth C, McLellan MD, Vandin F, Ye K, Niu B, Lu C, Xie M, Zhang Q, McMichael JF, and Wyczalkowski MA, et al (2013). Mutational landscape and significance across 12 major cancer types. *Nature* **502**(7471), 333–339.

[18] Hong MK, Macintyre G, Wedge DC, Van Loo P, Patel K, Lunke S, Alexandrov LB, Sloggett C, Cmero M, and Marass F, et al (2015). Tracking the origins and drivers of subclonal metastatic expansion in prostate cancer. *Nat Commun* **6**, 1–12. doi:10.1038/ncomms7605 6605.

[19] Bolli N, Avet-Loiseau H, Wedge DC, Van Loo P, Alexandrov LB, Martincorena I, Dawson KJ, Iorio F, Nik-Zainal S, and Bignell GR, et al (2014). Heterogeneity of genomic evolution and mutational profiles in multiple myeloma. *Nat Commun* **5**, 1–13. doi:10.1038/ncomms3997 2997.

[20] Maley CC, Galipeau PC, Finley JC, Wongsurawat VJ, Li X, Sanchez CA, Paulson TG, Blount PL, Risques RA, and Rabinovitch PS, et al (2006). Genetic clonal diversity predicts progression to esophageal adenocarcinoma. *Nat Genet* **38**(4), 468–473.

[21] Landau DA, Carter SL, Stojanov P, McKenna A, Stevenson K, Lawrence MS, Sougnez C, Stewart C, Sivachenko A, and Wang L, et al (2013). Evolution and impact of subclonal mutations in chronic lymphocytic leukemia. *Cell* **152**(4), 714–726.

[22] Kim H, Zheng S, Amini SS, Virk SM, Mikkelsen T, Brat DJ, Grimsby J, Sougnez C, Muller F, and Hu J, et al (2015). Whole-genome and multisector exome sequencing of primary and post-treatment glioblastoma reveals patterns of tumor evolution. *Genome Res* **25**(3), 316–327.

[23] Walker BA, Wardell CP, Melchor L, Brioli A, Johnson DC, Kaiser MF, Mirabella F, Lopez-Corral L, Humphray S, and Murray L, et al (2014). Intraclonal heterogeneity is a critical early event in the development of myeloma and precedes the development of clinical symptoms. *Leukemia* **28**(2), 384–390.

[24] Brioli A, Melchor L, Cavo M, and Morgan GJ (2014). The impact of intra-clonal heterogeneity on the treatment of multiple myeloma. *Br J Haematol* **165**(4), 441–454.

[25] Ding L, Raphael BJ, Chen F, and Wendl MC (2013). Advances for studying clonal evolution in cancer. *Cancer Lett* **340**(2), 212–219.

[26] Walter MJ, Shen D, Shao J, Ding L, White BS, Kandoth C, Miller CA, Niu B, McLellan MD, and Dees ND, et al (2013). Clonal diversity of recurrently mutated genes in myelodysplastic syndromes. *Leukemia* **27**(6), 1275–1282.

[27] Walker BA, Wardell CP, Melchor L, Hulkki S, Potter NE, Johnson DC, Fenwick K, Kozarewa I, Gonzalez D, and Lord CJ, et al (2012). Intraclonal heterogeneity and distinct molecular mechanisms characterize the development of t(4;14) and t(11;14) myeloma. *Blood* **120**(5), 1077–1086.

[28] Takatsuki K (2005). Discovery of adult T-cell leukemia. *Retrovirology* **2**, 16.

[29] Watanabe T (2017). Adult T-cell leukemia (ATL): molecular basis for clonal expansion and transformation of HTLV-1-infected T cells. *Blood* **129**(9), 1071–1081. doi:10.1182/blood-2016-09-692574.

[30] Gallo RC (2005). The discovery of the first human retrovirus: HTLV-1 and HTLV-2. *Retrovirology* **2**, 1–7. doi:10.1186/1742-4690-2-17.

[31] Tsukasaki K and Tobinai K (2013). Biology and treatment of HTLV-1 associated T-cell lymphomas. *Best Pract Res Clin Haematol* **26**(1), 3–14.

[32] Iwanaga M, Watanabe T, and Yamaguchi K (2012). Adult T-cell leukemia: a review of epidemiological evidence. *Front Microbiol* **3**, 1–13. doi:10.3389/fmicb.2012.00322 322.

[33] Tsukasaki K, Hermine O, Bazarbachi A, Ratner L, Ramos JC, Harrington Jr W, O'Mahony D, Janik JE, Bittencourt AL, and Taylor GP, et al (2009). Definition, prognostic factors, treatment, and response criteria of adult T-cell leukemia-lymphoma: a proposal from an international consensus meeting. *J Clin Oncol* **27**(3), 453–459.

[34] Firouzi S, Lopez Y, Suzuki Y, Nakai K, Sugano S, Yamochi T, and Watanabe T (2014). Development and validation of a new high-throughput method to investigate the clonality of HTLV-1-infected cells based on provirus integration sites. *Genome Med* **6**(6), 1–15. doi:10.1186/gm568 46.

[35] Farmanbar A, Firouzi S, Park SJ, Nakai K, Uchimaru K, and Watanabe T (2017). Multidisciplinary insight into clonal expansion of HTLV-1-infected cells in adult T-cell leukemia via modeling by deterministic finite automata coupled with high-throughput sequencing. *BMC Med Genomics* **10**(1), 1–12. doi:10.1186/s12920-016-0241-2 4.

[36] Aoki S, Firouzi S, Lopez Y, Yamochi T, Nakano K, Uchimaru K, Utusnomiya A, Iwanaga M, and Watanabe T (2016). Transition of adult T-cell leukemia/lymphoma clones during clinical progression. *Int J Hematol* **104**(3), 330–337.

[37] Farmanbar A, Firouzi S, Makalowski W, Iwanaga M, Uchimaru K, Utsunomiya A, Watanabe T, and Nakai K (2017). Inferring clonal structure in HTLV-1-infected individuals: towards bridging the gap between analysis and visualization. *Hum Genomics* **11**(1), 1–13. doi:10.1186/s40246-017-0112-8 15.

[38] Firouzi S, Farmanbar A, Nakai K, Iwanaga M, Uchimaru K, Utsunomiya A, Suzuki Y, and Watanabe T (2017). Clonality of HTLV-1-infected T-cells as a risk indicator for development and progression of adult T-cell leukemia. *Blood Adv* **1**(15).

[39] Turpin J, Alais S, Marcais A, Bruneau J, Melamed A, Gadot N, Tanaka Y, Hermine O, Melot S, and Lacoste R, et al (2017). Whole body clonality analysis in an aggressive STLV-1 associated leukemia (ATLL) reveals an unexpected clonal complexity. *Cancer Lett* **389**, 78–85.

[40] Yoshida N, Karube K, Utsunomiya A, Tsukasaki K, Imaizumi Y, Taira N, Uike N, Umino A, Arita K, and Suguro M, et al (2014). Molecular characterization of chronic-type adult T-cell leukemia/lymphoma. *Cancer Res* **74**(21), 6129–6138.

[41] Kataoka K, Nagata Y, Kitanaka A, Shiraishi Y, Shimamura T, Yasunaga J, Totoki Y, Chiba K, Sato-Otsubo A, and Nagae G, et al (2015). Integrated molecular analysis of adult T cell leukemia/lymphoma. *Nat Genet* **47**(11), 1304–1315.

[42] Casper J, Zweig AS, Villarreal C, Tyner C, Speir ML, Rosenbloom KR, Raney BJ, Lee CM, Lee BT, and Karolchik D, et al (2017). The UCSC Genome Browser database: 2018 update. *Nucleic Acids Res* **46**(D1), D762–D769. doi:10.1093/nar/gkx1020.

[43] Li H and Durbin R (2009). Fast and accurate short read alignment with Burrows-Wheeler transform. *Bioinformatics* **25**(14), 1754–1760.

[44] Li H, Handsaker B, Wysoker A, Fennell T, Ruan J, Homer N, Marth G, Abecasis G, Durbin R, and Genome Project Data Processing S (2009). The Sequence Alignment/Map format and SAMtools. *Bioinformatics* **25**(16), 2078–2079.

[45] McKenna A, Hanna M, Banks E, Sivachenko A, Cibulskis K, Kernytsky A, Garimella K, Altshuler D, Gabriel S, and Daly M, et al (2010). The Genome Analysis Toolkit: a MapReduce framework for analyzing next-generation DNA sequencing data. *Genome Res* **20**(9), 1297–1303.

[46] Sherry ST, Ward MH, Kholodov M, Baker J, Phan L, Smigielski EM, and Sirotkin K (2001). dbSNP: the NCBI database of genetic variation. *Nucleic Acids Res* **29**(1), 308–311.

[47] Wang K, Li M, and Hakonarson H (2010). ANNOVAR: functional annotation of genetic variants from high-throughput sequencing data. *Nucleic Acids Res* **38**(16), 1–7. doi:10.1093/nar/gkq603 e164.

[48] Koboldt DC, Zhang Q, Larson DE, Shen D, McLellan MD, Lin L, Miller CA, Mardis ER, Ding L, and Wilson RK (2012). VarScan 2: somatic mutation and copy number alteration discovery in cancer by exome sequencing. *Genome Res* **22**(3), 568–576.

[49] Seshan VE and Olshen A (2018). DNAcopy: DNA copy number data analysis. R package version 1.54.0; 2018. doi:10.18129/B9.bioc.DNAcopy.

[50] Mermel CH, Schumacher SE, Hill B, Meyerson ML, Beroukhim R, and Getz G (2011). GISTIC2.0 facilitates sensitive and confident localization of the targets of focal somatic copy-number alteration in human cancers. *Genome Biol* **12**(4), R41.

[51] Miller CA, White BS, Dees ND, Griffith M, Welch JS, Griffith OL, Vij R, Tomasson MH, Graubert TA, and Walter MJ, et al (2014). SciClone: inferring clonal architecture and tracking the spatial and temporal patterns of tumor evolution. *PLoS Comput Biol* **10**(8)e1003665.

[52] De Palma M and Hanahan D (2012). The biology of personalized cancer medicine: facing individual complexities underlying hallmark capabilities. *Mol Oncol* **6**(2), 111–127.

[53] Mroz EA, Tward AD, Hammon RJ, Ren Y, and Rocco JW (2015). Intra-tumor genetic heterogeneity and mortality in head and neck cancer: analysis of data from the Cancer Genome Atlas. *PLoS Med* **12**(2)e1001786.

[54] Lohr JG, Stojanov P, Carter SL, Cruz-Gordillo P, Lawrence MS, Auclair D, Sougnez C, Knoechel B, Gould J, and Saksena G, et al (2014). Widespread genetic heterogeneity in multiple myeloma: implications for targeted therapy. *Cancer Cell* **25**(1), 91–101.

[55] Anderson K, Lutz C, van Delft FW, Bateman CM, Guo Y, Colman SM, Kempski H, Moorman AV, Titley I, and Swansbury J, et al (2011). Genetic variegation of clonal architecture and propagating cells in leukaemia. *Nature* **469**(7330), 356–361.

[56] Johnson BE, Mazor T, Hong C, Barnes M, Aihara K, McLean CY, Fouse SD, Yamamoto S, Ueda H, and Tatsuno K, et al (2014). Mutational analysis reveals the origin and therapy-driven evolution of recurrent glioma. *Science* **343**(6167), 189–193.

[57] Govindan R (2014). Attack of the clones. *Science* **346**(6206), 169–170.

[58] Zhang J, Fujimoto J, Zhang J, Wedge DC, Song X, Zhang J, Seth S, Chow CW, Cao Y, and Gumbs C, et al (2014). Intratumor heterogeneity in localized lung adenocarcinomas delineated by multiregion sequencing. *Science* **346**(6206), 256–259.

[59] Utsunomiya A, Choi I, Chihara D, and Seto M (2015). Recent advances in the treatment of adult T-cell leukemia-lymphomas. *Cancer Sci* **106**(4), 344–351.

[60] Sakashita A, Hattori T, Miller CW, Suzushima H, Asou N, Takatsuki K, and Koeffler HP (1992). Mutations of the p53 gene in adult T-cell leukemia. *Blood* **79**(2), 477–480.

[61] Uchida T, Kinoshita T, Watanabe T, Nagai H, Murate T, Saito H, and Hotta T (1996). The CDKN2 gene alterations in various types of adult T-cell leukaemia. *Br J Haematol* **94**(4), 665–670.

[62] Kawano N, Shimoda K, Ishikawa F, Taketomi A, Yoshizumi T, Shimoda S, Yoshida S, Uozumi K, Suzuki S, and Maehara Y, et al (2006). Adult T-cell leukemia development from a human T-cell leukemia virus type I carrier after a living-donor liver transplantation. *Transplantation* **82**(6), 840–843.

[63] Yoshizumi T, Shirabe K, Ikegami T, Kayashima H, Yamashita N, Morita K, Masuda T, Hashimoto N, Taketomi A, and Soejima Y, et al (2012). Impact of human T cell leukemia virus type 1 in living donor liver transplantation. *Am J Transplant Off J Am Soc Transplant Am Soc Transplant Surg* **12**(6), 1479–1485.

[64] Yoshizumi T, Takada Y, Shirabe K, Kaido T, Hidaka M, Honda M, Ito T, Shinoda M, Ohdan H, and Kawagishi N, et al (2016). Impact of human T-cell leukemia virus type 1 on living donor liver transplantation: a multi-center study in Japan. *J Hepatobiliary Pancreat Sci* **23**(6), 333–341.

[65] Yoshida N, Miyoshi H, Kato T, Sakata-Yanagimoto M, Niino D, Taniguchi H, Moriuchi Y, Miyahara M, Kurita D, and Sasaki Y, et al (2016). CCR4 frameshift

mutation identifies a distinct group of adult T cell leukaemia/lymphoma with poor prognosis. *J Pathol* **238**(5), 621–626.

[66] Yoshie O, Fujisawa R, Nakayama T, Harasawa H, Tago H, Izawa D, Hieshima K, Tatsumi Y, Matsushima K, and Hasegawa H, et al (2002). Frequent expression of CCR4 in adult T-cell leukemia and human T-cell leukemia virus type 1-transformed T cells. *Blood* **99**(5), 1505–1511.

[67] Ishida T, Joh T, Uike N, Yamamoto K, Utsunomiya A, Yoshida S, Saburi Y, Miyamoto T, Takemoto S, and Suzushima H, et al (2012). Defucosylated Anti-CCR4 Monoclonal Antibody (KW-0761) for Relapsed Adult T-Cell Leukemia-Lymphoma: A Multicenter Phase II Study. *J Clin Oncol* **30**(8), 837–842.

[68] Yonekura K, Kanzaki T, Gunshin K, Kawakami N, Takatsuka Y, Nakano N, Tokunaga M, Kubota A, Takeuchi S, and Kanekura T, et al (2014). Effect of anti-CCR4 monoclonal antibody (mogamulizumab) on adult T-cell leukemia–lymphoma: Cutaneous adverse reactions may predict the prognosis. *J Dermatol* **41**(3), 239–244.

[69] Cleary AS, Leonard TL, Gestl SA, and Gunther EJ (2014). Tumour cell heterogeneity maintained by cooperating subclones in Wnt-driven mammary cancers. *Nature* **508**(7494), 113–117.

[70] Polyak K and Marusyk A (2014). Cancer: Clonal cooperation. *Nature* **508**(7494), 52–53.